

MODELING OF THE SIRIUS FAST ORBIT FEED-BACK CONTROL LOOP

IBIC 2024, BEIJING

L. A. PELIKE¹, J. C. S. CARVALHO¹, G. R. CRUZ¹, A. F. GIACHERO¹, A. C. S. OLIVEIRA¹, G. S. RAMIREZ¹, E. N. ROLIM¹, F. H. DE SÁ¹, D. O. TAVARES¹

¹Brazilian Synchrotron Light Laboratory (LNLS/CNPEM), Campinas, Brazil

PRESENTED BY:
LUCAS ANTONIO PELIKE

SEPTEMBER 11, 2024



MINISTRY OF
SCIENCE TECHNOLOGY
AND INNOVATION



- 1 SIRIUS's FOFB Overview
- 2 Control Loop Model
 - Basic Structure
 - Plant
 - Controller
 - Weighting matrices
- 3 System Identification
 - Experiments
 - Estimated Models
- 4 Model Evaluation
 - General Method
 - Open Loop
 - Sensitivity
 - MIMO
- 5 Conclusion
- 6 References

- 4th generation light source located in Brazil
- Storage ring circumference of 518.4 m and 3 GeV electron beam with currently 100 mA (350 mA nominal)
- Fast Orbit Feedback System (FOFB) currently employs 78 Fast Correctors (**156 coils**) and 80 BPMs (**160 BPM readings**)
- Orbit disturbance attenuation from 0.1 Hz to 1 kHz
- Update rate of 48 kHz
- In operation for users since 2022
- See article published in ICALEPCS 2023 [1] for technical details
- Objective: build a realistic computational model for the FOFB



Figure 1: SIRIUS light source

CONTROL LOOP MODEL - BASIC STRUCTURE

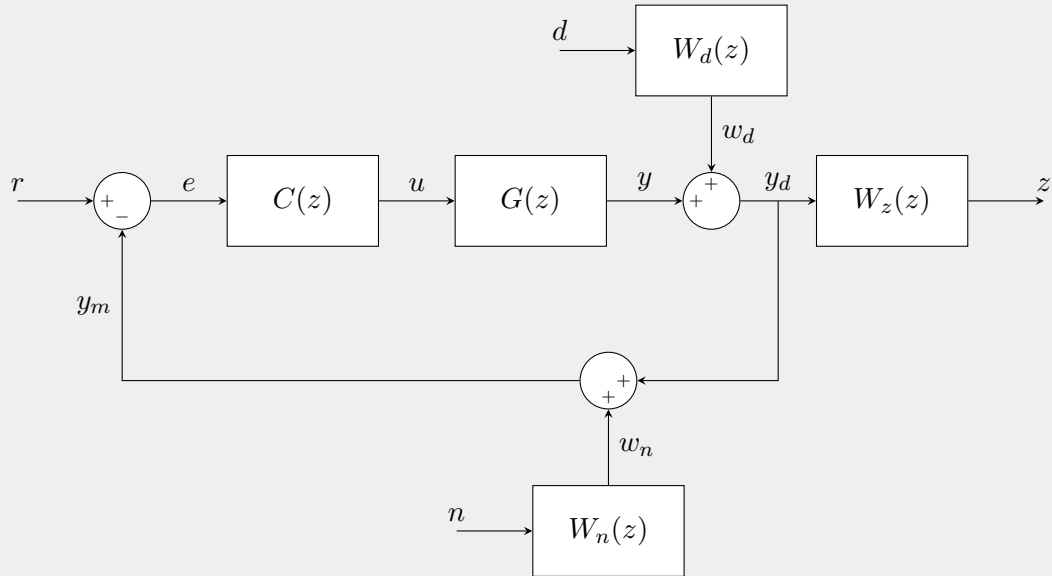


Figure 2: Control loop basic structure

CONTROL LOOP MODEL - PLANT

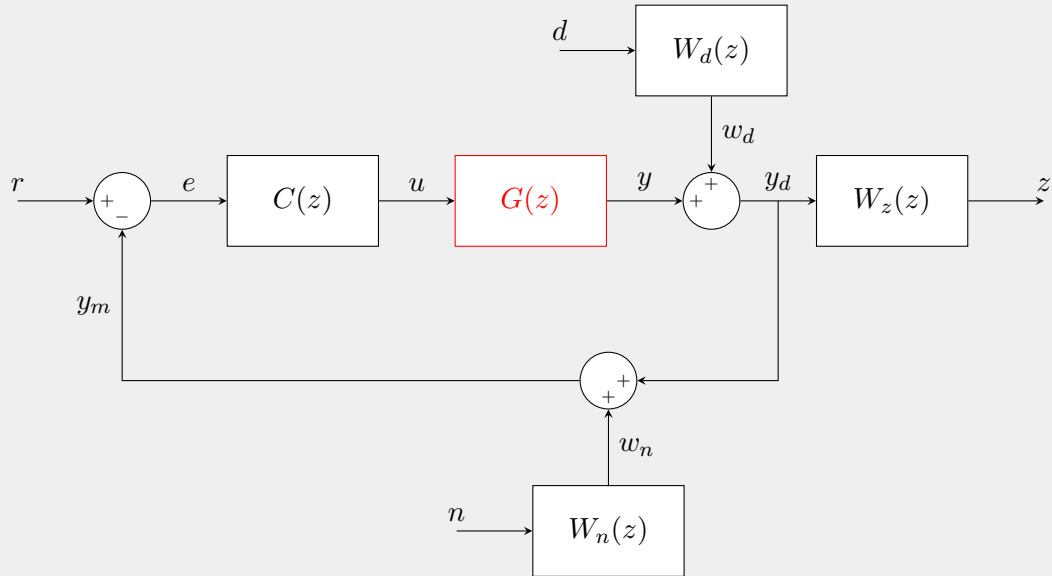


Figure 3: Plant

Plant $G(z)$

Constructed as

$$G(z) = [M \mid \eta] \left[\begin{array}{cccc} A_1(z) & \cdots & 0 & 0 \\ \vdots & \ddots & \vdots & \vdots \\ 0 & \cdots & A_n(z) & 0 \\ \hline 0 & \cdots & 0 & H(z) \end{array} \right]$$

where M is the measured Orbit Response Matrix, η is the dispersion column, $A_i(z)$ is the model for the i -th corrector and $H(z)$ models the phase to orbit transfer function. The general format for $H(z)$ may be found in [2].

CONTROL LOOP MODEL - CONTROLLER

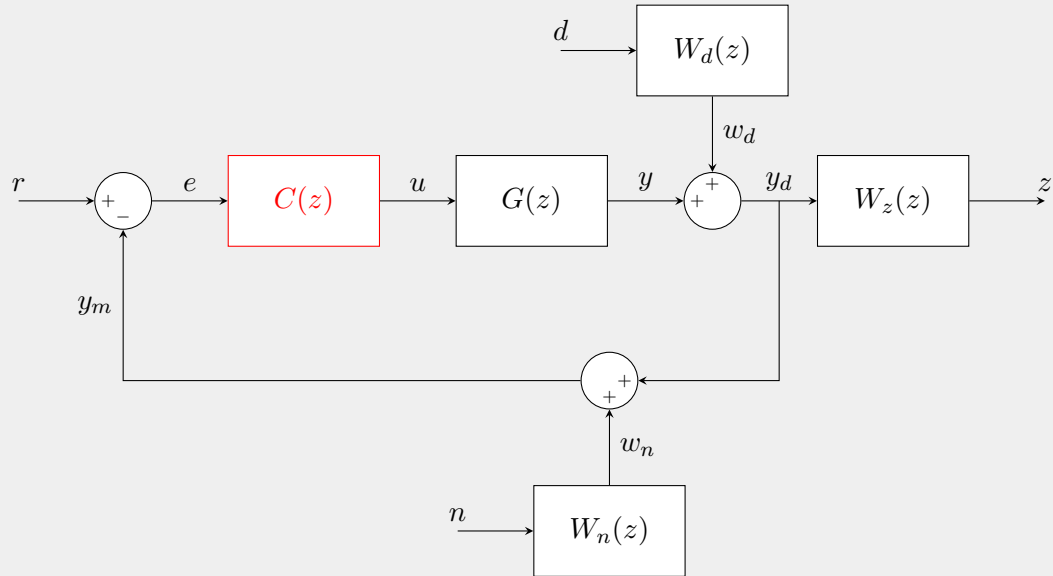


Figure 4: Controller

Controller $C(z)$

Basic integral controller, given by

$$C(z) = F(z) \left(K_I \frac{T_s z}{z - 1} \right) M_c$$

where $F(z)$ is an optional shaping filter, T_s is the sample period, M_c is a correction matrix (obtained from the pseudoinverse of the Orbit Response Matrix M) and K_I is a gain matrix, currently defined as

$$K_I = \begin{bmatrix} 0.120 & \cdots & 0 \\ \vdots & \ddots & \vdots \\ 0 & \cdots & 0.166 \end{bmatrix}$$

CONTROL LOOP MODEL - WEIGHTING MATRICES

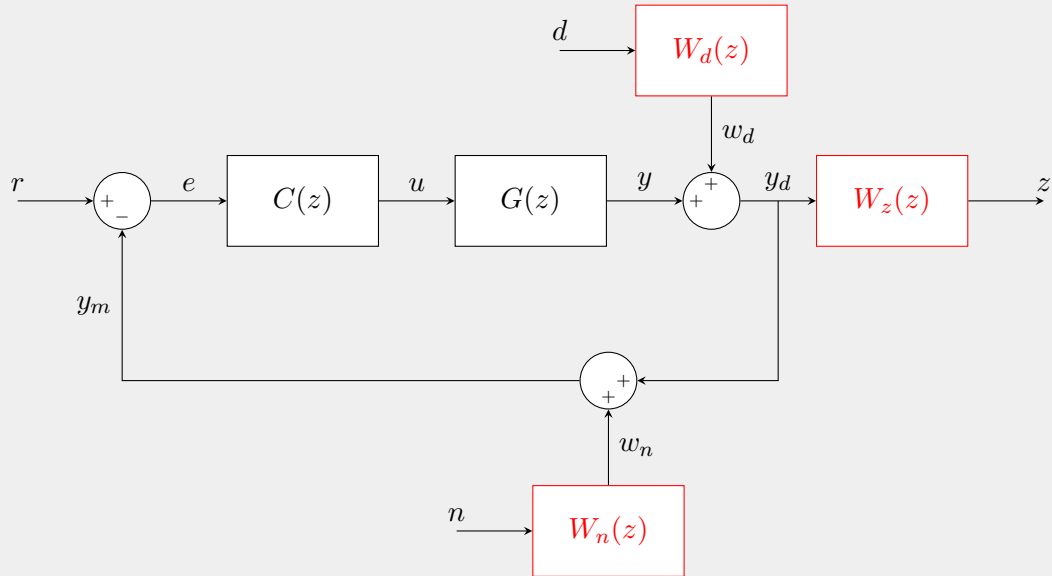


Figure 5: Weighting matrices

- Actuators' discrepancies motivated system identification experiments
- PRBS derived excitation signals
- Period of $N = 2^7 - 1 = 127$ steps and each applied step is composed of $d = 3$ equal applied samples
- 524 periods collected at a 48 kHz sampling rate and averaged to an equivalent sequence of a period with $Nd = 381$ samples
- Applied to correctors and measured at BPMs (zero gain applied to controller)

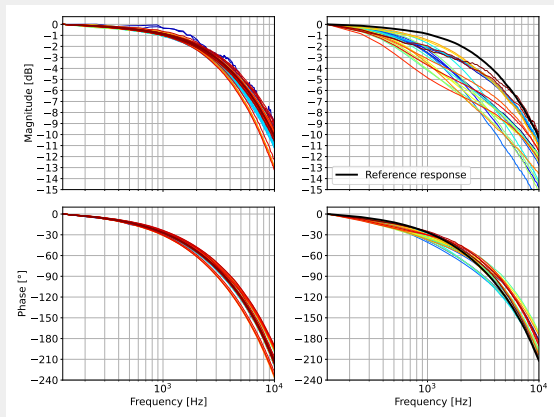


Figure 6: Frequency response of a subset of correctors [1].

- Plant system obtained with fits from experimental data
- Follows basic structure of [3]
- AutoRegressive with eXogenous inputs (ARX) models
- 6th degree polynomials and delay of 2 samples
- Reported fits above 90%
- Builds a system $A_i(z)$ for the i -th corrector. In our case, $1 \leq i \leq 156$

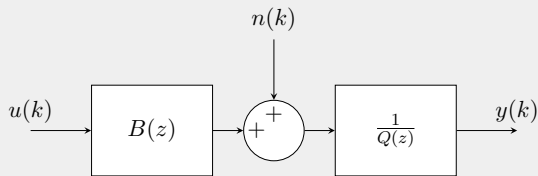


Figure 7: ARX basic structure

- Excited system's input with PRBS derived signals (parameters N and d)

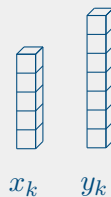


Figure 8: Input and output signals x_k and y_k , at sample $k \in \Lambda$, where Λ is an indexing set with Nd elements.

- Excited system's input with PRBS derived signals (parameters N and d)
- Sequence of matrices obtained from system response and excitation signal

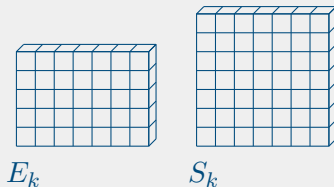


Figure 9: Building matrices E_k and S_k .

- Excited system's input with PRBS derived signals (parameters N and d)
- Sequence of matrices obtained from system response and excitation signal
- DFT of the projection to inputs and outputs of the obtained matrices

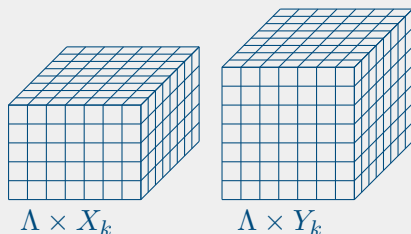


Figure 10: "FFT Cubes" obtained from joining the DFTs of input and output signals as columns.

- Excited system's input with PRBS derived signals (parameters N and d)
- Sequence of matrices obtained from system response and excitation signal
- DFT of the projection to inputs and outputs of the obtained matrices

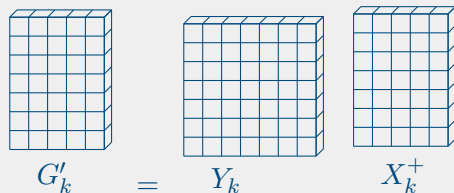


Figure 11: Computation of matrix G'_k evaluated at frequency sample k

- Excited each corrector with PRBS derived signals (parameters N and d)
- Sequence of matrices obtained from system response and excitation signal
- DFT of the projection to inputs and outputs of the obtained matrices
- Multiplication by the pseudoinverse and subsequent SVD from the resulting product

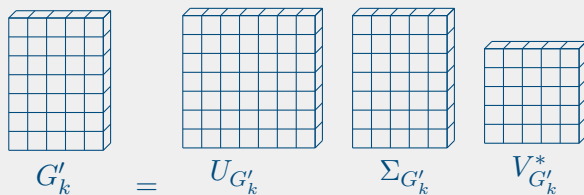


Figure 12: SVD of G'_k

- Excited system's input with PRBS derived signals (parameters N and d)
- Sequence of matrices obtained from system response and excitation signal
- DFT of the projection to inputs and outputs of the obtained matrices
- Multiplication by the pseudoinverse and subsequent SVD from the resulting product
- Allows one to identify singular values in frequency

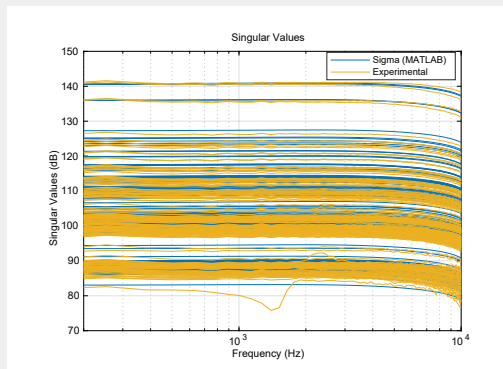


Figure 13: Open Loop singular values

- Essentially the same process as described
- Only one corrector and one BPM in the system
- System excitation at BPM readings
- Input signal with an amplitude of 5000 nm
- General agreement between model prediction and experimental data
- Crescent peak around 10 kHz is a consequence of the chosen d value

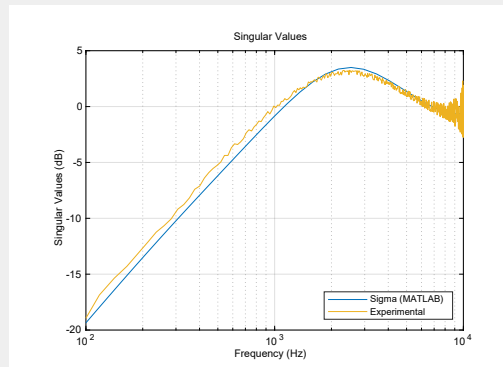


Figure 14: SISO singular values - horizontal

- Essentially the same process as in the MIMO case
- Only one corrector and one BPM in the system
- System excitation at BPM readings
- Input signal with an amplitude of 5000 nm
- General agreement between model prediction and experimental data
- Crescent peak around 10 kHz is a consequence of the chosen d value

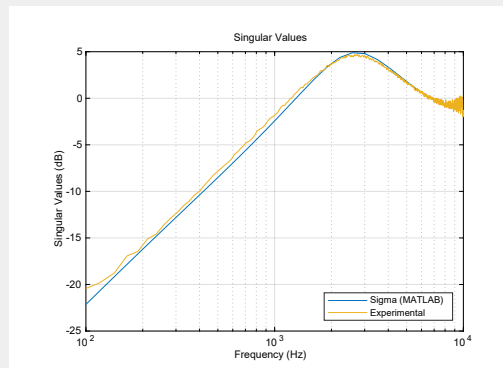


Figure 15: SISO singular values - vertical

MODEL EVALUATION - SENSITIVITY (MIMO)

- Simulated MIMO sensitivity using the model described
- Comparison between real model (unmatched correctors) and ideal (matched correctors)

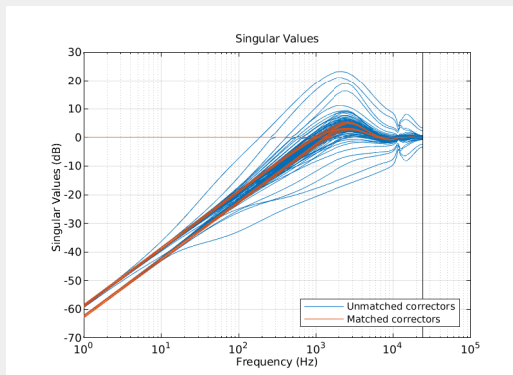


Figure 16: Simulated sensitivity for the obtained model.

- The proposed model allows a realistic analysis of SIRIUS's Fast Orbit Feedback by, for example, capturing discrepancies between fast correctors
- Noise and disturbance inputs allow us to analyze sensitivity and noise rejection for a given configuration
- Robustness considerations could be made by studying gain increases of the model
- An easy-to-use evaluation technique for the model was implemented
- Future work might be concentrated towards a better understanding of the interaction with LLRF loop and optimization tests with shaping filters

- [1] D.O. TAVARES ET AL. “**COMMISSIONING AND OPTIMIZATION OF THE SIRIUS FAST ORBIT FEEDBACK**”. In: *Proc. 19th Int. Conf. Accel. Large Exp. Phys. Control Syst. (ICALEPCS'23)* (Cape Town, South Africa, Oct. 9–13, 2023). International Conference on Accelerator and Large Experimental Physics Control Systems 19. JACoW Publishing, Geneva, Switzerland, Feb. 2024, pp. 123–130. ISBN: 978-3-95450-238-7. DOI: 10.18429/JACoW-ICALEPCS2023-M03A003. URL: <https://jacow.org/icalepcs2023/papers/mo3ao03.pdf>.
- [2] P. KALLAKURI ET AL. “**COUPLED BUNCH MODE ZERO CORRECTION USING ORBIT MEASUREMENTS AND RF SYSTEM PHASE FEEDBACK**”. In: *Physical Review Accelerators and Beams* 25.8 (Aug. 2022). ISSN: 2469-9888. DOI: 10.1103/physrevaccelbeams.25.082801. URL: <https://www.osti.gov/biblio/1882009>.
- [3] D. O. TAVARES AND D. R. GROSSI. “**SYSTEM IDENTIFICATION AND ROBUST CONTROL FOR THE LNLS UVX FAST ORBIT FEEDBACK**”. In: *Proc. ICALEPCS'15* (Melbourne, Australia, Oct. 2015). JACoW Publishing, Geneva, Switzerland, 2015, pp. 30–33. DOI: 10.18429/JACoW-ICALEPCS2015-M0C3004. URL: <https://jacow.org/ICALEPCS2015/papers/M0C3004.pdf>.

THANK YOU!